Microgrids for Enhancing the Power Grid Resilience in Extreme Conditions

Xindong Liu, Mohammad Shahidehpour, *Fellow, IEEE*, Zuyi Li, *Senior Member, IEEE*, Xuan Liu, *Member, IEEE*, Yijia Cao, *Senior Member, IEEE*, and Zhaohong Bie, *Senior Member, IEEE*

***Abstract*—This paper presents a framework for analyzing the resilience of an electric power grid with integrated microgrids in extreme conditions. The objective of this paper is to demonstrate that controllable and islandable microgrids can help improve the resiliency of power grids in extreme conditions. Four resilience indices are introduced to measure the impact of extreme events. Index *K* measures the expected number of lines on outage due to extreme events. Index loss of load probability measures the probability of load not being fully supplied. Index expected demand not supplied measures the expected demand that cannot be supplied. Index *G* measures the difficulty level of grid recovery. The mechanism of extreme events affecting power grid operation is analyzed based on the proposed mesh grid approach. The relationship among transmission grid, distribution grid, and microgrid in extreme conditions is discussed. The Markov chain is utilized to represent the state transition of a power grid with integrated microgrids in extreme conditions. The Monte Carlo method is employed to calculate the resilience indices. The proposed power grid resilience analysis framework is demonstrated using the IEEE 30-bus and 118-bus systems assuming all loads are within microgrids.**

***Index Terms*—Power system operation, resilience, microgrids, extreme events.**

NOMENCLATURE

Indices and Sets

i, j	General indices
t	Index for times
S_e	Set of extreme events
S_m	Set of Markov state spaces.

Variables

C_{π_i}	Load curtailment in state π_i
$EDNS$	Expected demand not supplied
f	Fragility distribution function in extreme conditions
G	Grid recovery index
k	Number of lines on outage
K	Expected number of lines on outage
L_Ω	Load curtailment in extreme conditions without microgrids
$LOLP$	Loss of load probability
p_{ij}	Probability of state transition from state i to state j
P_{e_i}	Probability of power grid in state e_i
P_d	Probability of k lines on outage
T_{e_i}	Duration of power grid in state e_i
V	Severity level of extreme condition
w	Weight of factor contributing to recovery index
η	Value of factor contributing to recovery index
λ_{ij}	Failure rate from state i to state j
μ_{ij}	Repair rate from state i to state j
π_j	Probability of state j in Markov chain process
π	Stationary distribution of Markov chain process.

Manuscript received July 13, 2015; revised November 25, 2015, January 21, 2016, and April 16, 2016; accepted June 8, 2016. Date of publication June 10, 2016; date of current version February 16, 2017. This work was supported by the National Natural Science Foundation of China under Grant 51377072, Grant 51307071, and Grant 51137003. Paper no. TSG-00816-2015.

X. Liu is with the College of Electrical and Information and the Institute of Rail Transportation, Jinan University, Zhuhai 519000, China (e-mail: baiom@126.com).

M. Shahidehpour is with the Galvin Center for Electricity Innovation, Illinois Institute of Technology, Chicago, IL 60616 USA, and also with the Renewable Energy Research Group, King Abdulaziz University, Jeddah 21589, Saudi Arabia (e-mail: ms@iit.edu).

Z. Li is with the Galvin Center for Electricity Innovation, Illinois Institute of Technology, Chicago, IL 60616 USA.

X. Liu is with the Electrical Engineering Department, Chongqing University, Chongqing 400044, China.

Y. Cao is with the College of Electrical and Information Engineering, Hunan University, Changsha 410006, China.

Z. Bie is with the State Key Laboratory of Electrical Insulation and Power Equipment and the School of Electrical Engineering, Xi'an Jiaotong University, Xi'an 710049, China.

Color versions of one or more of the figures in this paper are available online at http://ieeexplore.ieee.org.

Digital Object Identifier 10.1109/TSG.2016.2579999

I. INTRODUCTION

POWER transmission and distribution facilities are exposed to numerous adverse effects in broad geographical areas where hazardous conditions can appear frequently. A reliable and secure operation is a prerequisite for a resilient power system which can survive in extreme conditions [1]–[5]. Power system reliability evaluations are focused on adequacy and security analyses [6]. Adequacy is the ability to supply power system loads continuously. Security is the ability to withstand sudden disturbances such as the unexpected loss of power system components [7]. In comparison, reliability is related to events with a high probability but a relatively low impact (such as power system faults) whereas resilience is related to events with a low probability but a high impact (such as hurricanes and tornados). The difference between reliability and resilience is demonstrated by the survivability of power systems when experiencing extreme events [8].

Microgrids, which are represented as controllable loads in power systems, combine local energy assets and demand response for managing the smart grid in various conditions. The resilience benefits are analyzed in [9] and [10]. In [11], the power grid resilience is improved by optimally controlling

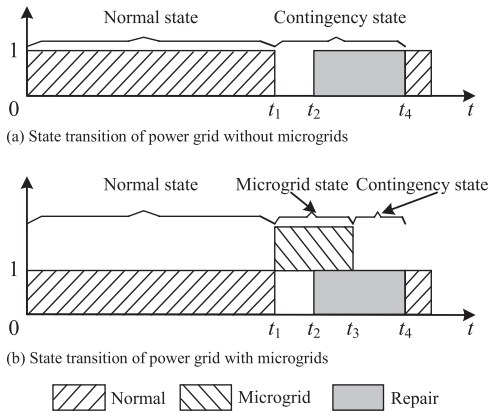

Fig. 1. Power grid operation states without and with microgrids.

fixed and adjustable loads, dispatchable and non-dispatchable units and energy storage units in microgrids. Microgrids usually cover small geographical areas within distribution networks, and distribution networks in turn represent buses in large transmission networks. Power grids integrated with a large number of microgrids would incur less load curtailments in extreme conditions. Thus, critically-situated and largely-aggregated microgrids would sustain the supply of power to local loads through self-healing and islanding strategies, which can improve the power grid resilience within specified time intervals.

Extreme events such as hurricanes can disrupt daily operations of electricity infrastructures with unprecedented consequences. Extreme events are surveyed and the costs of mitigation strategies that leverage distributed resources are summarized in [12] and [13]. Microgrids, which can be operated in island mode, are frequently considered as key elements for enhancing the grid resilience. In addition, grid-connected microgrids which are often considered for peak load reductions can also enhance the large-scale grid reliability [14]. In [15], microgrids are introduced as an effective means of reconfiguring power grid operations rapidly as the grid gets subjected to severe outages. By deploying a critical number of microgrids in strategic geographical locations, power grid operation can be enhanced during major outages [16].

Various models and indices are developed recently for evaluating the power grid resilience. The resilience in the communication network protocol is quantified by a radar plot [17]. The resilience of networked systems during extreme conditions was analyzed considering the interdependency of electricity and telecommunication infrastructures [18]. Reference [19] formulated a resilience index for large infrastructures using belief functions and proposed a variety of qualitative explanations to address and analyze the power grid vulnerability.

The three operation states (i.e., normal state, contingency state and microgrid state) shown in Fig. 1 illustrate the impact of microgrid deployment. In Fig. 1(a), an extreme event occurs at time t_1 which interrupts the power supply; the restoration is started at t_2 which is completed at t_4. The states would be different when microgrids are deployed. In Fig. 1(b), the microgrid starts to work in island mode at t_1. The supply of local loads powered by microgrids is interrupted when the available fuels are depleted at t_3. In this circumstance, we can enhance the grid resilience by equipping microgrids with distributed generation that would extend the supply of local power through t_4. By deploying microgrids, the interruption time is reduced from t_4-t_1 to t_4-t_3. Case studies in this paper provide the additional details for similar resilience cases.

The contributions of this paper are listed as follows. A framework is presented for analyzing the resilience of an electric power grid with integrated microgrids in extreme conditions. Four resilience indices are introduced to measure the impact of extreme events. The mechanism of extreme events affecting power grid operation is analyzed based on a mesh grid approach. The Markov chain is utilized to represent the state transition of a power grid with integrated microgrids in extreme conditions. The Monte Carlo method is employed to calculate the resilience indices. In this paper, we build the relationship between utilizing multiple microgrids and the grid resiliency by employing the Markov model and the Monte Carlo simulation approach, which can be used for both reliability and risk evaluations in power systems.

II. Resilience Indices and Resilience Analysis Framework

Four indices are introduced in this paper to measure the grid resilience from different perspectives including fragility, survivability and recovery. In particular, index K measures the expected number of lines on outage due to extreme events. Index Loss of load probability (*LOLP*) measures the probability of load not being fully supplied. Index expected demand not served (*EDNS*) measures the expected demand that cannot be supplied. Index G measures the difficulty level of grid recovery. Accordingly, the power grid resilience metric is stated as $\Theta = \{K, LOLP, EDNS, G\}$.

The fragility function f, which characterizes the probability of outages corresponding to a certain extreme event, is presented as

$$f = P_d(k|V) \tag{1}$$

$$K = \int_0^\infty kf(k)dk \tag{2}$$

where k is the number of lines on outage, V refers to the severity level of extreme events, P_d is the probability of k line outages in V, f denotes the fragility distribution. Index K represents the expected number of lines on outage due to extreme events in level V.

Two traditional reliability indices including the *LOLP* and *EDNS* [14] are modified in our study to describe the power grid survivability following extreme events

$$LOLP = \sum_{e_i \in S_e} P_{e_i} \tag{3}$$

$$EDNS = \sum_{e_i \in S_e} P_{e_i} C_{e_i} \tag{4}$$

where e_i represents the i^{th} extreme event, P_{e_i} is the probability of power grid experiencing e_i, S_e is the set of extreme

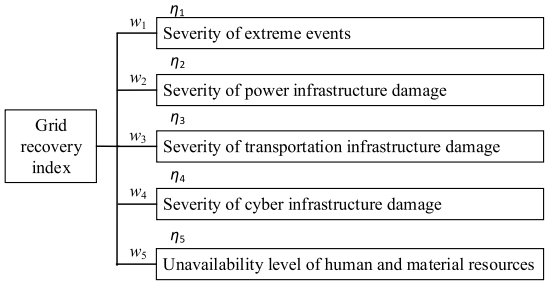

Fig. 2. Composition of grid recovery index.

events in which the system load exceeds the available generating capacity. C_{e_i} is the load curtailment in e_i, which can be calculated by the optimal power flow (OPF) solution and may include strategic load shedding in microgrids.

The power supply restoration process in extreme events may take several hours or even days, depending on the severity of the extreme events, and the extent of damages to critical infrastructures including power, transportation, and cyber infrastructures. The improved weather forecasting and situational awareness in extreme conditions may be able to contain the severity of damages to the critical infrastructures and mobilize organizational human and material resources for a comprehensive recovery of the power grid. Here, the power grid recovery index is different from the traditional mean time to repair (MTTR), which in most cases depends on the state of equipment on outage. The proposed grid recovery index is described in Fig. 2 and expressed as

$$G = \sum_{i=1}^{5} w_i \eta_i \tag{5}$$

$$\sum_{i=1}^{5} w_i = 1 \tag{6}$$

where w_i and η_i are the weight and value of the i-th factor that affects the grid recovery index G.

Fig. 3 show the proposed framework for grid resilience analyses in extreme conditions in power grids which are integrated with microgrids. The framework includes two parts. In Part A, the statistics of extreme events and microgrids are analyzed for the initial modeling of extreme conditions. The power grid operations in extreme conditions are significantly different than those of cascading failures or typical N-1 failures. Extreme events usually cover several geographical areas in major outages. Besides, an extreme event usually has a low probability of occurrence in which several transmission lines or subsystems would be on outage simultaneously. Furthermore, microgrids usually offer a more viable option when operated in island mode, which would greatly improve the resilience of power grids. The power grid control strategy and performance depend significantly on the deployment of microgrids in a large-scale power grid. For instance, when isolated from the power grid, microgrids with sufficient fuel supplies can survive longer than other segments of the power grid which lack the necessary resources for survival.

Therefore, the coordination between microgrid runtimes (i.e., available operation time) and the power grid recovery

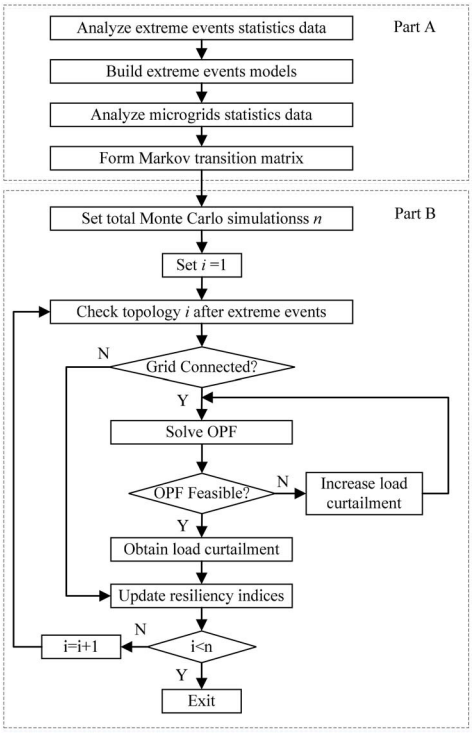

Fig. 3. Framework for resilience analyses of power grids with microgrids.

process plays an important role in power grid resilience. The statistical analyses of microgrid availability in island mode are critical for quantifying the power grid resilience as extreme events occur. Accordingly, the relationship between power grid and microgrid are introduced in Section III and a Markov state transition matrix is introduced in Section IV to compute the respective probabilities of corresponding operating states.

In Part B, the Monte Carlo approach is adopted to calculate the power grid resilience indices. The connectivity of power grid is analyzed when the topology is altered after an extreme event. If the network connectivity is maintained, an OPF is performed to check whether the grid can operate within its limits. If the OPF solution is infeasible, a pre-defined load curtailment schedule is pursued (e.g., system loads are reduced by 5% at a time). Also, a more sophisticated methodology can be taken into account to minimize load curtailments. The resilience indices are then updated in each Monte Carlo simulation.

III. Relationship of Transmission and Distribution Grids With Microgrids

According to the Reliability Report published by the Edison Electric Institute (EEI) in 2008, 67% of electrical outage minutes in the U.S. were weather related in which the restoration service cost exceeded $2.7 billion in 2005 [13]. The extreme events such as the Superstorm Sandy in the U.S. in 2012 affected 24 states with an estimated damage of $65 billion [13].

Fig. 4 depicts several examples of extreme events that affected the electricity infrastructure in large areas with varied intensities. Fig. 4(a) is the image of the Great Blizzard of 1993 [20]. Fig. 4(b) is the image of Hurricane Katrina in

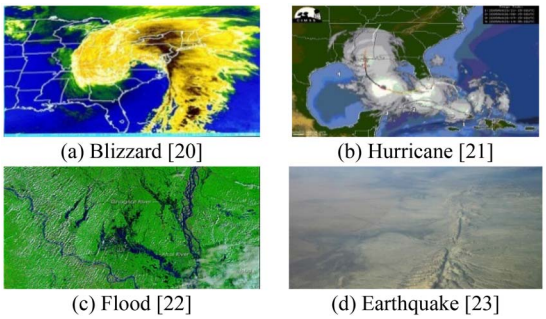

Fig. 4. Samples of extreme events.

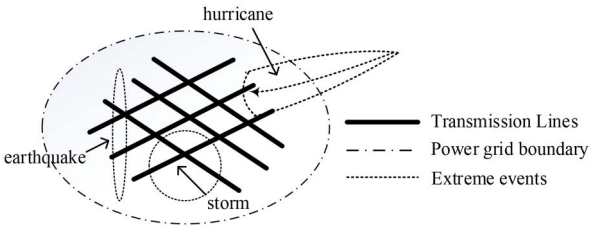

Fig. 5. Interaction of extreme events and power grid.

2005 [21]. Fig. 4(c) is the image of the flooded Ghaghat and Atral Rivers in 2005 [22]. Fig. 4(d) is the aerial photo of the San Andreas Fault in the Carrizo Plain, northwest of Los Angeles [23].

The broader scope of extreme events can be abstracted with a geometric sketch in Fig. 5, where transmission lines, grid boundary, and extreme events are represented by solid, dash-dotted, and dotted lines, respectively. Hurricanes, blizzards, and earthquakes are depicted as parabolic, circular, and elliptical curves, respectively. Here, transmission line outages can be followed via geometric paths of extreme events on power grids. The interactions of extreme events and the power grid can accordingly be regarded as an *N-K* problem, where *K* is the expected number of lines on outage resulting from extreme events. The number of lines on outage would depend on the degree of damages to the power grid caused by extreme events.

In practice, the geographic information system (GIS) integrated with a transmission line layer can be employed to find the impact of line outages in extreme events. Alternatively, the mesh view of a power grid shown in Fig. 6 is adopted in this paper. Here, the IEEE 30-bus system [24] is illustrated in a mesh grid with $8*12 = 96$ cells. Each cell on the mesh can be represented by its coordinates such as Cell(3,7). When an extreme event occurs, its center and boundaries would be represented in shaded colors as in Fig. 6. The lines connecting buses 15 and 23, and buses 23 and 24 in Cell(3,7) would be tripped with a higher probability, and the lines connecting buses 15 and 18, buses 18 and 19, and buses 21 and 22 in Cell(3,6), Cell(4,6), Cell(4,7), Cell(4,8), and Cell(3,8) would be tripped with a lower probability. Correspondingly, the interactions of extreme events and the power grid in this case is represented as an "N-K" problem. We can increase the mesh granularity in Fig. 6. For example, if the mesh dimensions are doubled in both horizontal and vertical directions, the mesh

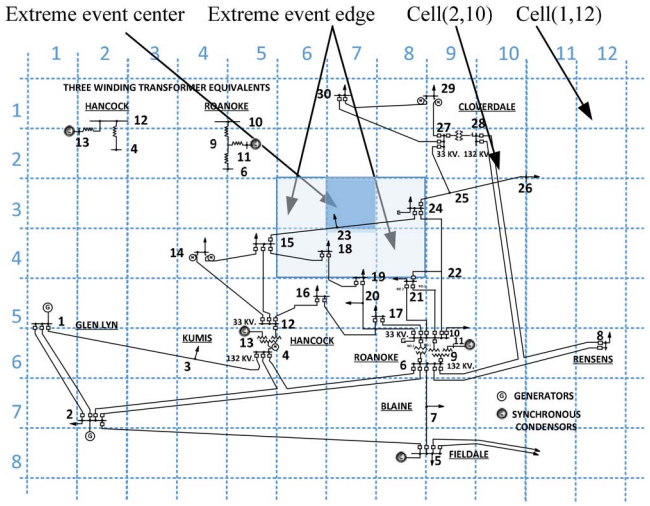

Fig. 6. Mesh view of the IEEE 30-bus system.

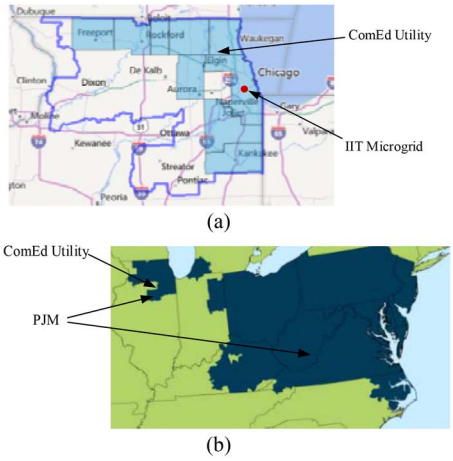

Fig. 7. IIT microgrid, ComEd utility grid, and PJM power grid.

grid for the IEEE 30-bus system would be represented by $(8*2)*(12*2) = 384$ cells.

An extreme event could cover an area that is hundreds of square kilometers wide in practical systems, while a microgrid, with an area of a few square kilometers, would represent a small portion of the large power grid. The comparison of the Illinois Institute of Technology (IIT) microgrid, ComEd utility grid, and PJM power grid are shown in Fig. 7. In Fig. 7(a), the IIT microgrid is depicted as a small portion of the ComEd utility grid. In Fig. 7(b), the ComEd utility grid is represented as a fraction of the PJM power grid. The extreme events, such as the blizzard in Fig. 4(a), can interrupt the transmission flow in the PJM power grid and further affect the supply of power to the ComEd utility grid. The deployment of several microgrids in the ComEd utility grid can potentially curb the load curtailment and improve the grid resilience in the event of major outages.

The relationship among transmission and distribution grid and microgrid are illustrated and a detailed load model is depicted in Fig. 8. The transmission lines in Fig. 8 interconnect transmission loads (TL). A TL usually consists of distribution networks, distribution loads (DLs), and microgrids.

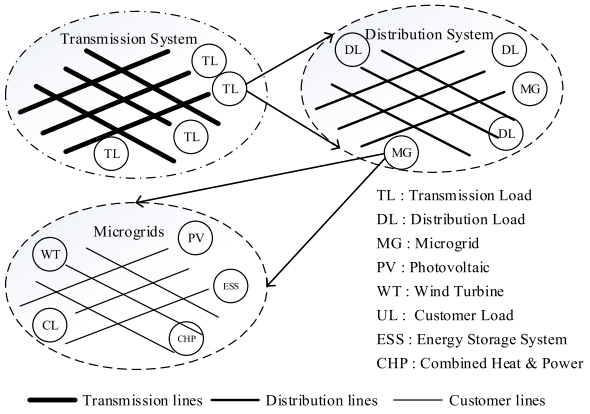

Fig. 8. Relationship among transmission, distribution and microgrid systems.

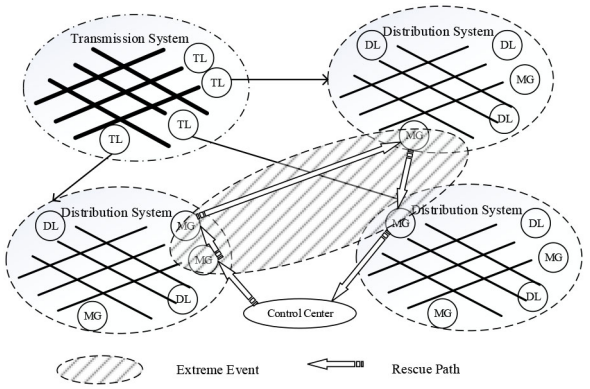

Fig. 9. An example of recovery strategy.

The grid-connected microgrids in Fig. 8 are eventually regarded as DLs which possess various forms of onsite distributed energy resources (DERs) including photovoltaic generation (PV), wind turbine generation (WT), small hydro generation (SH), combined heat & power generation (CHP), energy storage system (ESS), and customer load (CL). These DERs are combined through elaborated control strategies to operate the system as a microgrid.

The TLs in Fig. 8 can easily be affected by extreme events with large scale impacts, further interrupting the power supply to distribution systems and degrading the power grid resilience. However, the depicted microgrid loads can be maintained in island mode by utilizing local DERs and in turn improving the system resilience in extreme conditions. We address in the following section the grid resilience using a wider perspective and build the relationship among transmission, distribution, and microgrid systems for discussing the grid resilience.

The proposed methodology in this paper is applied to measure the grid resilience and help improve the recovery responses to extreme events, such as the ability to resist, the ability to adapt, and the time to recover from disruptions. For instance, in Fig. 9, the extreme event affects four microgrids, which are located in three distribution systems and reflected as three nodes at the transmission level. The control center would dispatch rescue resources to the affected microgrid areas. At the recovery stage, the system rescue path usually depends

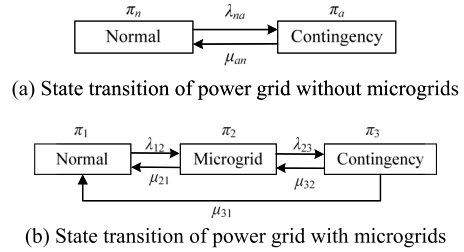

(a) State transition of power grid without microgrids

(b) State transition of power grid with microgrids

Fig. 10. State transition of power grid without and with microgrids.

on tangible issues such as the minimum outage time or rescue cost. The resilience analysis when considering microgrids may change the rescue path and reduce the outage time. In Fig. 9, suppose the runtime of individual microgrids in island mode is given. Accordingly, we can shorten the rescue path and reduce the total outage time of the system by first rescuing those microgrids which have shorter runtimes. Here, by optimizing the rescue path in distribution systems with microgrids, we demonstrate that power grids which utilize microgrids can potentially be more resilient than those without microgrids.

IV. Power Grid State Transition Analyses

The extreme events that hit a power grid could inevitably require time-consuming and costly repairs. However, individual microgrids can offer their specific availability for supplying loads in extreme conditions. Large amounts of microgrids integrated in distribution systems can enhance the resiliency of transmission system. The state transition analysis of a power grid integrated with a large number of installed microgrids considers the coordination of the two entities in such occasions. In this paper, the control of microgrid loads is considered as a fundamental element of grid resilience analyses, as aggregated microgrid loads represent the bus loads in larger power grids.

Without considering microgrids, power grid operation states are divided into normal and contingency states as shown in Fig. 10(a). The system will transition to a contingency state with a failure rate λ_{na} in extreme conditions and return to the normal state with a repair rate μ_{an}. The failure and repair rates can be obtained based on historical data of extreme events and the corresponding power grid recovery times.

State transitions will change dramatically when microgrids are integrated in power grids as shown in Fig. 10(b). In extreme conditions, the power grid state will change from the normal state to the microgrid state with a failure rate λ_{12} when microgrid loads are supplied by local DERs in island mode. The power grid will then return to the normal state with a repair rate μ_{21} or to the contingency state with a failure rate λ_{23}, according to the microgrid availability and the grid recovery times. In the contingency state, the power grid will return to the microgrid state with a repair rate μ_{32} or the normal state with a repair rate μ_{31}, depending on the grid recovery strategy. Some typical values for μ and λ can be found in [25].

The state transition in Fig. 10 is a Markov chain process [26]–[28]. The process of a time-homogeneous

Markov chain can be characterized by a time-independent matrix P, in which π_j, the probability of each state j, satisfies (7)-(9).

$$0 \le \pi_j \le 1 \tag{7}$$

$$\sum_{j \in S} \pi_j = 1 \tag{8}$$

$$\pi_j = \sum_{i \in S_m} \pi_i p_{ij} \tag{9}$$

Based on the steady-state analysis and limiting distribution property [25], a stationary distribution $\pi = [\pi_1, \pi_2, \ldots, \pi_j]$ is related to the state transition matrix P by

$$\pi P = \pi \tag{10}$$

Eq. (10) is further represented as

$$\pi (P - I) = 0 \tag{11}$$

The state transition matrix P corresponding to Fig. 10(b) is

$$P = \begin{bmatrix} 1-\lambda_{12} & \lambda_{12} & 0 \\ \mu_{21} & 1-\mu_{21}-\lambda_{23} & \lambda_{23} \\ \mu_{31} & \mu_{32} & 1-\mu_{31}-\mu_{32} \end{bmatrix} \tag{12}$$

Substituting (12) into (11) and transposing the equation, we have,

$$\begin{bmatrix} -\lambda_{12} & \mu_{21} & \mu_{31} \\ \lambda_{12} & -\mu_{21}-\lambda_{23} & \mu_{32} \\ 0 & \lambda_{23} & -\mu_{31}-\mu_{32} \end{bmatrix} * \begin{bmatrix} \pi_1 \\ \pi_2 \\ \pi_3 \end{bmatrix} = 0 \tag{13}$$

According to (8),

$$\pi_1 + \pi_2 + \pi_3 = 1 \tag{14}$$

Solving (13) and (14), we can obtain π_1, π_2 and π_3 as,

$$\pi_1 = \frac{\mu_{21}(\mu_{31}+\mu_{32}) + \mu_{31}\lambda_{23}}{\lambda_{23}(\mu_{31}+\lambda_{12}) + (\mu_{21}+\lambda_{12})(\mu_{31}+\mu_{32})} \tag{15}$$

$$\pi_2 = \frac{\lambda_{12}(\mu_{31}+\mu_{32})}{\lambda_{23}(\mu_{31}+\lambda_{12}) + (\mu_{21}+\lambda_{12})(\mu_{31}+\mu_{32})} \tag{16}$$

$$\pi_3 = \frac{\lambda_{12}\lambda_{23}}{\lambda_{23}(\mu_{31}+\lambda_{12}) + (\mu_{21}+\lambda_{12})(\mu_{31}+\mu_{32})} \tag{17}$$

where π_1, π_2 and π_3 are the steady-state probabilities for normal, microgrid, and emergency states, respectively. The changes in failure and repair rates lead to different steady-state probabilities, offering an intuitive perspective of the power system reliability. With the above probabilities, the load curtailment in extreme events is given as,

$$C_{e_i} = \frac{\pi_3}{\pi_2 + \pi_3} * L_\Omega \tag{18}$$

where L_Ω is the load curtailment due to extreme events without considering microgrids. Accordingly, *EDNS* is updated as follows based on (4).

$$EDNS = \sum_{e_i \in S_e} P_{e_i} * \frac{\pi_3}{\pi_2 + \pi_3} * L_\Omega \tag{19}$$

V. Case Studies

In this section, extreme events are simulated for the IEEE 30-bus and IEEE 118-bus systems in order to illustrate the proposed grid resilience analysis framework.

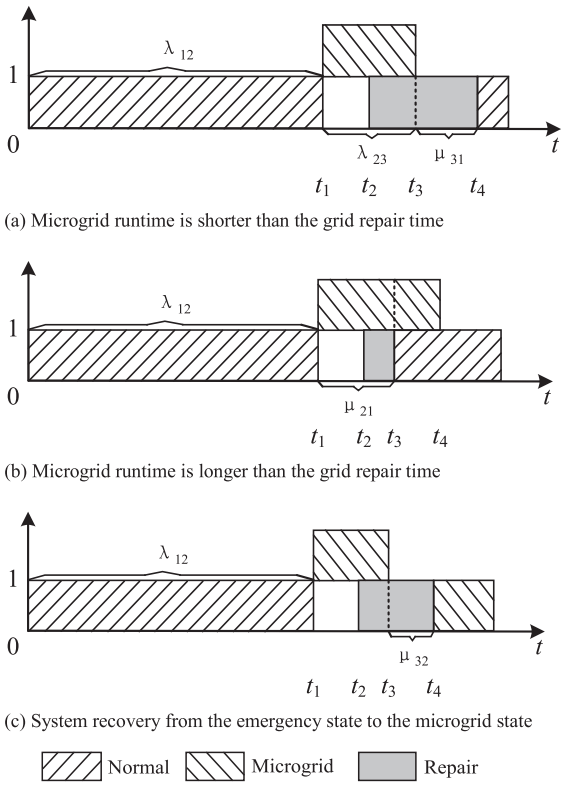

Fig. 11. Statistics of state transitions for power grid integrated with microgrids.

TABLE I
Statistics for Power Grids and Microgrid Operations

Parameter	Related statistical time duration	value
λ_{12}	1 years	1
λ_{23}	1 week	52.1
μ_{21}	2 weeks	26.1
μ_{32}	3 weeks	17.38
μ_{31}	3 weeks	17.38

A. Simulation Parameters

Fig. 11 shows the state transition of a power grid integrated with microgrids. The parameters $\lambda_{(.)}$ *and* $\mu_{(.)}$ shown in Fig. 11 do not measure the durations; however, they are computed using the corresponding durations. In Fig. 11(a), the grid switches from the normal state to the microgrid state after an extreme event and then changes to the emergency state (i.e., grid repair) when microgrids fail to operate (e.g., due to fuel shortages). Parameters λ_{23} and μ_{31} are presented using Fig. 11(a). In Fig. 11(b), microgrids run longer than the duration of grid repair and the microgrid island mode is terminated at time t_3, when parameter μ_{21} can be obtained. In Fig. 11(c), the microgrid runs out of fuel, and the system switches to emergency state at time t_3; the system returns to the microgrid state at time t_4, when parameter μ_{32} can be obtained. Parameter λ_{12} is calculated from the sum of system runtimes in normal state in Figs. 11 (a)-(c).

Suppose the statistical time durations for calculating λ and μ are listed in Table I. Then λ_{12}, which provides the grid failure rate due to extreme events, is 1/1=1; λ_{23}, which represents the failure rate of microgrids, is 1/(7/365)=52.1. Similarly, μ_{21},

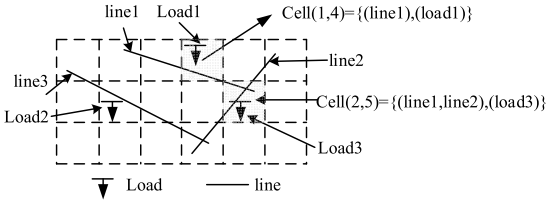

Fig. 12. Mesh grid format of power grid geographic diagram.

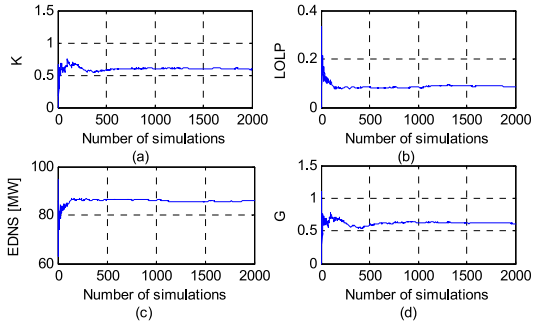

Fig. 13. Simulation results for extreme events covering a small area.

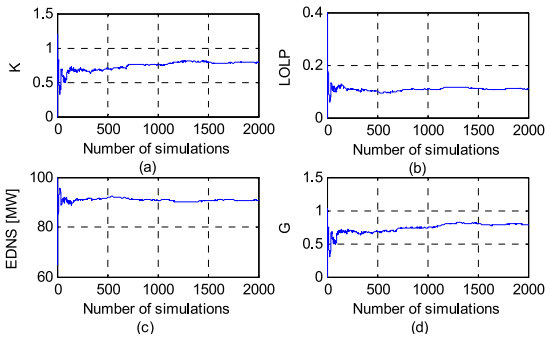

Fig. 14. Simulation results for extreme events in a large geographical area.

μ_{32}, and μ_{31} are listed as 26.1, 17.38 and 17.38, respectively. According to (15)-(17), the steady-state probabilities of individual states based on the historical data are $\pi_1 = 0.9586$, $\pi_2 = 0.0276$ and $\pi_3 = 0.0138$. The weights w_1 - w_5 in Fig. 2 for calculating the grid recovery index are all set to 0.2. The values of the five factors η_1 - η_5 are all set to the expected number of line outages. They can be set according to Fig. 2 for a real system if corresponding information is available.

B. IEEE 30 Bus-System

To illustrate the resilience of the power grid integrated with microgrids, a mesh grid is considered for the IEEE 30-bus system [24], as shown in Fig. 6. Each cell has an attribute to represent loads and transmission lines. Take Fig. 12 as an example. Cell(1,4) includes {(line1), (load1)}, and Cell(2,5) includes {(line1, line2), (load3)}. Power lines and loads in a cell will be tripped if extreme events occur inside that cell.

Suppose that all loads can be deployed within microgrids. Also assume that PV and wind turbine generators in a microgrid are tripped due to severe weather. The maximum number of simulations in the Monte Carlo method is set to 2000. The random extreme events vary within the range of 1 to 2 cells in

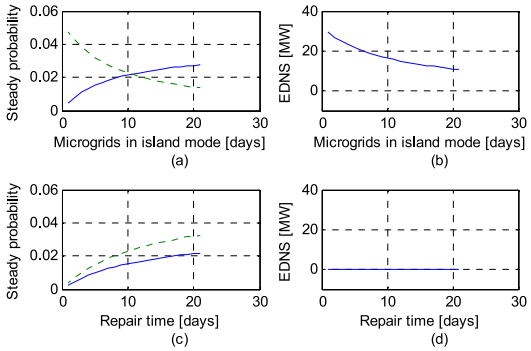

Fig. 15. Steady state probability analyses and expected load curtailments.

the mesh grid. The MATPOWER software [29] is utilized for OPF calculations. Figs. 13 and 14 show the Monte Carlo simulation results when extreme events cover a small and a large area, respectively.

Resilience index *K*, which is the expected number of line trips due to the random extreme events is 0.58 in Fig. 13(a) and 0.8 in Fig. 14(a). With a larger area affected by extreme events, the connectivity to a larger portion of the network is lost. Accordingly, resilience index *LOLP*, which is the probability of load not being fully supplied, is up from 0.09 in Fig. 13(b) to 0.14 in Fig. 14(b); and resilience index *EDNS*, which is the expected load curtailment, is up from 88 MW in Fig. 13(c) to 92 MW in Fig. 14(c). Resilience index *G*, which is the grid recovery index, changes from 0.58 in Fig. 13(d) to 0.8 in Fig. 14(d), which means a more extensive repair is needed when the extreme events cover a larger area. It is observed that all resilience indices, including the average number of line trips (*K*), connectivity losses (*LOLP*), and load curtailments (*EDNS*), and the grid recovery index (*G*) will increase with more intensive extreme events.

The probabilities for microgrid and contingency states and the corresponding expected load curtailments as a function of microgrid runtime and grid repair times are illustrated in Fig. 15. Figs. 15(a)-(b) represent the situation when the microgrid runtime is shorter than the grid repair time while Figs. 15(c)-(d) show the reverse case when the grid repair time is shorter than the microgrid runtime.

In Figs. 15(a) and (c), solid and dashed lines are the probabilities of microgrid states and contingency states, respectively. The probability of microgrid states will increase while the probability of contingency states will decrease as the microgrid runtime increases, as shown in Fig. 15(a). The corresponding expected load curtailment will also decrease, as shown in Fig. 15(b). In Fig. 15(c), both the probabilities of microgrid and contingency states will increase with the increasing repair time. Fig. 15(d) shows that the expected load curtailment will be zeroes if microgrids with long runtimes are deployed. Accordingly, a low cost and long repair time will not affect the expected load curtailment in a power grid which is integrated with long lasting microgrids.

C. IEEE 118 Bus-System

The IEEE 118-bus system [30] as shown in Fig. 16 includes 19 generators, 177 transmission lines, and 91 loads. The system is divided into two areas and the one within the rectangle

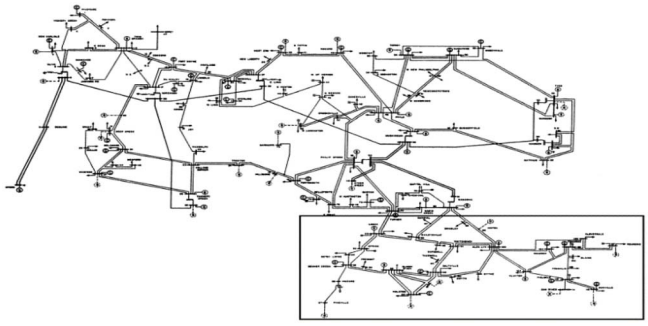

Fig. 16. One-line diagram of the IEEE 118-bus system.

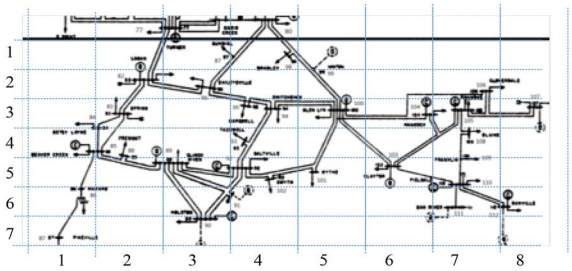

Fig. 17. Mesh grid of the selected area for the IEEE 118-bus system.

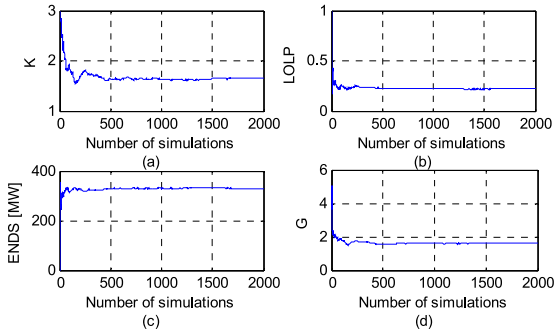

Fig. 18. Simulation results for extreme events in the IEEE 118-bus system.

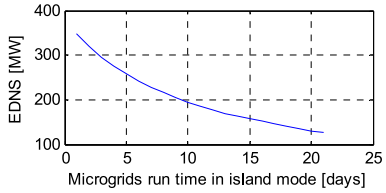

Fig. 19. Expected load curtailment with increasing microgrid runtimes.

is selected for analysis in the paper. Suppose the selected area is represented by a 7*8 = 56 mesh grid shown in Fig. 17. Also assume that the random extreme events cover only one cell at a time.

The Monte-Carlo simulation results are shown in Fig. 18. The *K* index is 1.7 as shown in Fig. 18(a) and the *LOLP* index is 0.22 as shown in Fig. 18(b). These two values are larger than those in Figs. 13-14 due to a larger area coverage of the extreme events thus more intensive damages to the power grid. The *EDNS* index in Fig. 18(c) is only 330MW. The *G* index in Fig. 18(d) is 1.7, which is larger than those in Figs. 13-14 (smaller than 1). It means that it is more difficult for the system to recover.

As shown in Fig. 19, the expected load curtailment drops when microgrids with long runtime are deployed in power grids.

VI. Conclusion

The extreme events have become more prevalent which pose greater challenges to the resilience of electric power grids. Microgrids represent a key component in power grid for improving the grid resilience. This paper has modeled the extreme events and analyzed the state transition of power grids integrated with microgrids. The paper has proposed four indices for measuring the resilience of power grids under extreme conditions. By interpreting the interactions among extreme events, power grid, and microgrids, the proposed framework represents an effective way of analyzing the resilience of large power grids by leveraging smart grid technologies in extreme conditions. This paper signifies a critical starting point for addressing the complex issue of quantifying the grid resilience in extreme conditions. The future work may include the sensitivity of grid resilience to the number of regional microgrids, and the power grid survivability when a large number of microgrids are islanded simultaneously.

References

[1] M. Roach, "Community power and fleet microgrids: Meeting climate goals, enhancing system resilience, and stimulating local economic development," *IEEE Electrific. Mag.*, vol. 2, no. 1, pp. 40–53, Mar. 2014.

[2] L. Che, M. Khodayar, and M. Shahidehpour, "Only connect: Microgrids for distribution system restoration," *IEEE Power Energy Mag*., vol. 12, no. 1, pp. 70–81, Jan./Feb. 2014.

[3] S. H. Liu, Y. H. Hou, C.-C. Liu, and R. Podmore, "The healing touch: Tools and challenges for smart grid restoration," *IEEE Power Energy Mag.*, vol. 12, no. 1, pp. 54–63, Jan./Feb. 2014.

[4] X. D. Liu, M. Shahidehpour, Y. J. Cao, Z. Li, and W. Tian, "Risk assessment in extreme events considering the reliability of protection systems," *IEEE Trans. Smart Grid*, vol. 6, no. 2, pp. 1073–1081, Mar. 2015.

[5] M. Amin, "Toward self-healing energy infrastructure systems," *IEEE Comput. Appl. Power*, vol. 14, no. 1, pp. 20–28, Jan. 2001.

[6] W. Y. Li, *Risk Assessment of Power Systems*. Hoboken, NJ, USA: Wiley, Mar. 2006, p. 4.

[7] (Oct. 2015). *Reliability*. [Online]. Available: http://www.energy.kth.se/compedu/webcompedu/Glossary/R/Reliability.htm

[8] (Oct. 2015). *Grid Resiliency*. [Online]. Available: http://www.epri.com/Pages/Grid-Resiliency.aspx

[9] M. Shahidehpour and S. Pullins, "Microgrids, modernization, and rural electrification," *IEEE Electrific. Mag.*, vol. 3, no. 1, pp. 2–6, Mar. 2015.

[10] L. Che, M. Shahidehpour, A. Alabdulwahab, and Y. Al-Turki, "Hierarchical coordination of a community microgrid with AC and DC microgrids," *IEEE Trans. Smart Grid*, vol. 6, no. 6, pp. 3042–3051, Nov. 2015.

[11] A. Khodaei, "Resiliency-oriented microgrid optimal scheduling," *IEEE Trans. Smart Grid*, vol. 5, no. 4, pp. 1584–1591, Jul. 2014.

[12] R. Arghandeh *et al.*, "The local team: Leveraging distributed resources to improve resilience," *IEEE Power Energy Mag*., vol. 12, no. 5, pp. 76–83, Sep./Oct. 2014.

[13] (Jan. 2015). *Enhancing Distribution Resiliency: Opportunities for Applying Innovative Technologies*. [Online]. Available: http://tdworld.com/site-files/tdworld.com/files/archive/tdworld.com/go-grid optimization/distribution/1026889EnhanceDistribution Resiliency.pdf

[14] (Oct. 2015). *Energy Surety Microgrid*. [Online]. Available: http://energy.sandia.gov/energy/ssrei/gridmod/integrated-research-and-development/esdm/

[15] N. Abi-Samra, J. McConnach, S. Mukhopadhyay, and B. Wojszczyk, "When the bough breaks: Managing extreme weather events affecting electrical power grids," *IEEE Power Energy Mag*., vol. 12, no. 5, pp. 61–65, Sep./Oct. 2014.
[16] L. Che and M. Shahidehpour, "DC microgrids: Economic operation and enhancement of resilience by hierarchical control," *IEEE Trans. Smart Grid*, vol. 5, no. 5, pp. 2517–2526, Sep. 2014.
[17] O. Erdene-Ochir, A. Kountouris, M. Minier, and F. Valois, "A new metric to quantify resiliency in networking," *IEEE Commun. Lett.*, vol. 16, no. 10, pp. 1699–1702, Oct. 2012.
[18] D. A. Reed, K. C. Kapur, and R. D. Christie, "Methodology for assessing the resilience of networked infrastructure," *IEEE Syst. J.*, vol. 3, no. 2, pp. 174–180, Jun. 2009.
[19] N. O. Attoh-Okine, A. T. Cooper, and S. A. Mensah, "Formulation of resilience index of urban infrastructure using belief functions," *IEEE Syst. J.*, vol. 3, no. 2, pp. 147–153, Jun. 2009.
[20] (Jan. 2015). *The Great Blizzards*. [Online]. Available: http://yourweatherblog.com/?p=837
[21] (Jan. 2015). *Hurricane Katrina*. [Online]. Available: http://www.earthlyissues.com/katrina.htm
[22] (Jan. 2015). *Flood*. [Online]. Available: http://en.wikipedia.org/wiki/Flood
[23] (Jan. 2015). *Earthquake*. [Online]. Available: http://en.wikipedia.org/wiki/Earthquake
[24] (Jan. 2015). *Power Systems Test Case Archive*. [Online]. Available: http://www.ee.washington.edu/research/pstca/pf30/pg_tca30bus.htm
[25] R. Billinton and R. Allan, *Power System Reliability Evaluation*. New York, NY, USA: Springer, 1996.
[26] (Jan. 2015). *Markov Chain*. [Online]. Available: https://en.wikipedia.org/wiki/ Markov_chain
[27] S. M. Iyer, M. K. Nakayama, and A. V. Gerbessiotis, "A Markovian dependability model with cascading failure," *IEEE Trans. Comput.*, vol. 58, no. 9, pp. 1238–1249, Sep. 2009.
[28] B. Hua, Z. H. Bie, S.-K. Au, W. Y. Li, and X. F. Wang, "Extracting rare failure events in composite system reliability evaluation via subset simulation," *IEEE Trans. Power Syst.*, vol. 30, no. 2, pp. 753–762, Mar. 2015.
[29] (Jan. 2015). *MATLAB Power System Simulation Package*. [Online]. Available: http://www.pserc.cornell.edu//matpower/
[30] (Jan. 2015). *Illinois Center for Smarter Electric Grid (ICSEG)*. [Online]. Available: http://publish.illinois.edu/smartergrid/case-6-ieee-118-bus-systems

Xindong Liu received the M.S. and Ph.D. degrees from Zhejiang University, Hangzhou, China, in 2006 and 2009, respectively. He is currently an Associate Professor with the College of Electrical and the Information and Institute of Rail Transportation, Jinan University, Zhuhai, China, and a Visiting Professor with the Illinois Institute of Technology. His current research interests include power system risk assessment, power system stability and control, and smart grid.

Mohammad Shahidehpour (F'01) received the Honorary Doctorate degree from the Polytechnic University of Bucharest, Bucharest, Romania. He is the Bodine Chair Professor and the Director of the Robert W. Galvin Center for Electricity Innovation, Illinois Institute of Technology, Chicago, IL, USA. He is also a Research Professor with King Abdulaziz, Saudi Arabia. He was a recipient of the IEEE PES Douglas M. Staszesky Distribution Automation Award and the IEEE PES Outstanding Educator Award. He is a member of the U.S. National Academy of Engineering.

Zuyi Li (SM'09) received the B.S. degree from Shanghai Jiaotong University, the M.S. degree from Tsinghua University, and the Ph.D. degree from the Illinois Institute of Technology (IIT), in 1995, 1998, and 2002, all in electrical engineering. He is currently a Full Professor with IIT. His research interests include economic and secure operation of electric power systems, cyber security in smart grid, renewable energy integration, and power system protection.

Xuan Liu (M'14) received the B.S. and M.S. degrees from Sichuan University, China, in 2008 and 2011, respectively, and the Ph.D. degree from the Illinois Institute of Technology, Chicago, in 2015, all in electrical engineering. He is currently a Faculty Member with the Electrical Engineering Department, Chongqing University. His research interests include smart grid security, operation, and economics of power systems.

Yijia Cao (SM'14) received the Ph.D. degree from the Huazhong University of Science and Technology, Wuhan, China, in 1994. He is currently a Professor and the Vice President with Hunan University. His main research interest is smart grid and power system risk assessment.

Zhaohong Bie (SM'98) received the Ph.D. degree from Xi'an Jiaotong University, Xi'an, China, in 1998. She is currently a Professor in the State Key Laboratory of Electrical Insulation and Power Equipment and the School of Electrical Engineering, Xi'an Jiaotong University. Her main interests and research fields are power system planning and reliability evaluation as well as the integration of the renewable energy.